

Effect of 4A zeolite on adsorption and release properties of sodium alginate/chitosan microspheres to sodium valproate

W. Y. Chen, X. J. Jiao, Y. F. Liu, J. X. Liu, B. H. Zhang*

Institute of New Pesticide Innovation & Research, Qingdao Agricultural University, Qingdao, People's Republic of China

4A zeolite/sodium alginate/chitosan microspheres (4A/SA/CS Ms) and sodium alginate/chitosan microspheres (SA/CS Ms) were prepared and its characterization were confirmed by the results of XRD, FTIR and SEM. Results showed that the addition of 4A zeolite can enlarge its particle size and is more conducive to balling. Adsorption properties of two microspheres toward sodium valproate (SV) were studied at different pH and temperature and it can be observed that the equilibrium adsorption capacity of 4A/SA/CS Ms for SV at pH = 7 was 8.1833 mg/g, compared with 4.9776 mg/g by SA/CS Ms, which reveal that 4A zeolite can increase the adsorption capacity. Cumulative release percentage reach to 42.69% in 48 hours by 4A/SA/CS@SV Ms at 25 °C and pH = 7 which demonstrated that 4A zeolite could improve the drug release performance. Overall, these results suggest that 4A/SA/CS Ms show a case to be used as promising drug carriers.

(Received May 12, 2022; Accepted August 25, 2022)

Keywords: 4A zeolite, Sodium valproate (SV), Microspheres (Ms), Adsorption, Release

1. Introduction

The present traditional pesticide formulations are generally toxic, high dosage and low efficiency, seriously polluting the environment and endangering human health[1-3]. SV has the advantages of broad anti-epileptic spectrum and good efficacy, and is an effective drug for the treatment of epilepsy, which is widely used in clinical medicine[4-6]. Song et al. demonstrated that SV also has good inhibitory activity against a variety of plant pathogenic fungi and bacteria through indoor toxicity measurements[7], indicating that SV can be used as a fungicide in agricultural production. As a bactericide, SV has the advantages of high efficiency, low toxicity and environmental friendliness which is suitable for the requirements of chemical control of plant diseases. It is safe for non target organisms and meets the requirements of sustainable development, so its research and market application prospects are broad[8-9]. As we all know, SV is prone to deliquesce and difficult to achieve long-term effect[10-11], which greatly reduces its bactericidal function. Now, sustained-release agent plays an increasingly prominent role in agriculture which has the characteristics of convenient use, good internal absorption performance and easy control. If SV can be made into a controlled-release formulation, it can release its effect slowly over time, saving labor and material resources, thus reducing residues in the environment and achieving

* Corresponding author: zhangbaohua76@163.com

sustainable development in agriculture.

Sodium alginate is linked by β -D-mannuronic acid and α -L-guluronic acid and it is biodegradable, low toxicity and low cost, which makes it suitable for biomedicine, pharmaceutical preparations and other fields. Large amount of $-\text{COO}^-$ in sodium alginate makes it show polyanion behavior in aqueous solution so it can rapidly form gelatin under extremely mild conditions[12-14]. When Ca^{2+} , Sr^{2+} and other cations exist, Na^+ in the molecule will react with two valence cations to form a cross-linked network structure, resulting in a hydrogel that can be used as a drug carrier for the treatment of mucosal tissues. Moreover, with high moisture content, good degradability and compatibility, sodium alginate polymers have been widely used in the development of pesticide controlled release dosage forms[15-17]. Chitosan is prepared from chitin by deacetylation reaction to remove acetyl group which is non-toxic, good film-forming, biocompatible[18-20]. Additionally chitosan can be made into microspheres or microcapsules because of its film forming performance, so it is extensively employed as a bio-material carrier owing to its unique properties[21-24]. 4A zeolite is a three-dimensional skeleton structure compound composed of silica and alumina tetrahedron and it has large pore structure, specific surface area, strong adsorption performance and skeleton support[25-26]. Currently, 4A zeolite is applied in chemical industry, environmental protection, agriculture and many other fields. In agriculture, 4A zeolite can be used as a soil conditioner to adjust the pH of soil, for instance, it can be combined with ammonium salt, rare earth elements or trace elements to make fertilizer slow-release agent[27-29]. Therefore, 4A zeolite has the application value as a controlled-release material.

Our previous study showed that 4A zeolite significantly improved the performance of sodium alginate/chitosan microspheres[30]. And the addition of 4A zeolite could effectively inhibit the excessive swelling of microspheres and reduce the number of microspheres break. In this work, 4A zeolite/sodium alginate/chitosan microspheres (4A/SA/CS Ms) and sodium alginate/chitosan microspheres (SA/CS Ms) SV-loaded were prepared. Furthermore, in order to reveal the effects of 4A zeolite on the properties of microspheres and lay the foundation for the application of the microspheres as a carrier of SV, the adsorption and release behavior of SV on two microspheres were also studied in different pH and temperature. Therefore, the purpose of this study was to find a suitable carrier for SV that can potentially be utilized in sustained-release agent.

2. Experimental

2.1. Materials

4A Zeolite were purchased from Alfa Aesar (Product of United States); Chitosan (CS, deacetylation degree 80%-90%, $\text{MW} \geq 100,000 \text{ g} \cdot \text{mol}^{-1}$) were purchased from Sinopharm Chemical Reagent Co. Ltd. (Beijing, China); Sodium alginate (SA, the molecular weight was around 30 kDa) was obtained from Tianjin Bodi Chemical Co., Ltd; 2-sodium valproate (>98.0%, AR), purchased from Aladdin Industrial Corporation; Calcium chloride (AR), Disodium hydrogen phosphate (AR), Acetonitrile (AR), Acetic acid (AR), Sodium hydroxide (AR), Potassium bromide (AR), all these reagents were purchased from Tianjin BASF Chemical Co., Ltd; Ultra pure water (AR), Weifang Wahaha Beverage Co., Ltd; Other chemicals and reagents are commercially available and were used directly.

2.2. Experimental

2.2.1. Preparation of 4A/SA/CS microspheres

The 4A/SA/CS Ms were prepared by a complex coacervation method similar to the procedure reported previously [30]. Firstly, 1.5 g of sodium alginate was dissolved in 50 mL of deionized water, followed by adding 1.5 g 4A zeolite evenly. Then, draw up the above solution with a 2.5 mL syringe (5# needle), with the needle perpendicular to the surface of the liquid, and slowly add dropwise into 50 mL of 30 g/L calcium chloride solution. Calcification for 30 minutes followed by filtration, the collected precipitate was then added to 50 mL of chitosan solution (20 g/L) and stirred for 30 minutes. After filtration, the collected product was then washed with distilled water three times and dried (air-dried, freeze-dried) to obtain 4A/SA/CS Ms.

2.2.2. Preparation of SA/CS microspheres

The SA/CS Ms were prepared in a way similar to that of the 4A/SA/CS Ms synthesis except for the absence of 4A zeolite addition.

2.2.3. Preparation of drug loaded microspheres

A certain amount of microspheres was dispersed in 30 mL of SV solution (solvent is water) shaking at different temperatures (10 °C, 25 °C, 40 °C) and pH (pH = 5, 7, 9) to obtain drug-loaded microspheres. After filtering and drying to a constant weight, the drug-loaded microspheres were stored in a centrifuge tube and kept away from light, which named as SA/CS Ms@SV and 4A/SA/CS Ms@SV, respectively.

2.2.4. Adsorption study

According to the method of preparing drug loaded microspheres in 2.2.3, different concentration of SV were mixed with different microspheres in 250mL brown vials. All bottles were shaken at 150 r/min at 25 °C. About 0.1 mL of supernatant was extracted at different time and the taken upper liquid is filtered through a filter membrane with a pore diameter of 0.22 μm and the concentration of SV was measured by HPLC[31]. The experiments were run in duplicate and the mean of results was calculated.

Thermodynamic parameters of SV adsorption by different microspheres at different temperatures were described by the following equation. Then, the thermodynamic parameters of the adsorption, i.e. the equilibrium constants (K_d) (1), the standard Gibbs free energy ΔG , enthalpy ΔH , and entropy ΔS , were calculated from the Van't Hoff Eq. (2), The slope and the intercept of the plots of $\ln K_d$ versus $1/T$ (3)[32] were used to determine the ΔH and ΔS values:

$$K_d = q_e/C_e \quad (1)$$

$$\Delta G = -RT \ln K_d \quad (2)$$

$$\ln K_d = -\Delta H/RT + \Delta S/R \quad (3)$$

Here: K_d is the adsorption equilibrium constant (mL/g); R is the ideal gas constant, 8.314 J/(mol·K); T is the thermodynamic temperature (K).

Two typical kinetic models (pseudo-first-order and pseudo-second-order) equations are expressed by equation (4) and equation (5)[33] respectively and the equilibrium adsorption rate

constant were calculated.

$$\log(q_e - q_t) = \log q_e - k_1 t / 2.303 \quad (4)$$

$$t/q_t = t/q_e + 1/k_2 q_e^2 \quad (5)$$

Here: k_1 and k_2 are adsorption rate constants (h^{-1}); t is the adsorption time (h), q_t is the adsorption capacity of t time (mg/g), q_e is the adsorption capacity at equilibrium.

Langmuir equation (6) and Freundlich equation (7)[34] are used to fit the adsorption thermodynamics. The fitting equation is as follows:

$$C_e/q_e = C_e/q_{\max} + 1/(q_{\max} * K_L) \quad (6)$$

$$\ln q_e = \ln k_F + (1/n) * \ln C_e \quad (7)$$

Here: q_{\max} is the maximum adsorption capacity of complete monolayer coverage (mg/g); k_L is the constant indirectly related to the adsorption capacity and adsorption energy (mL/mg); k_F is a constant, which is used to represent the adsorption capacity; n is a constant, indicating the adsorption strength.

2.2.5. Release study

Place SA/CS Ms@SV or 4A/SA/CS Ms@SV in a triangular flask containing 30 mL of ultrapure water, oscillate for different times (5 min, 10 min, 30 min, 1 h, 2 h, 4 h, 8 h, 12 h, 24 h, 32 h, 48 h), rotating speed 150 rpm. At different times, take 0.1 mL of upper liquid and add 0.1 mL of ultrapure water at the same time. The taken upper liquid is filtered through a filter membrane with a pore diameter of 0.22 μm and the peak area measured by HPLC. Draw the desorption kinetic curve and calculate the content of SV released from SA/CS Ms@SV or 4A/SA/CS Ms@SV, meanwhile, calculate the cumulative release percentage according to formula (8)[35]:

$$CRP\% = \frac{V \sum_{i=1}^{n-1} C_i + V_0 C_n}{m_0} \times 100\% \quad (8)$$

Therein: CRP is the cumulative release percentage, %; V is the volume of solution taken out (0.1 mL); V_0 is the volume of adsorbed solution (30 mL); C_i is the mass concentration of SV in the solution at the moment before C_n , mg/mL; m_0 is the mass of SV adsorbed in the microspheres, mg.

The release mechanism of two kinds of microspheres toward SV was researched by fitting drug release model. The commonly used fitting models include first-order drug release model, such as formula (9), Higuchi equation, formula (10) and Riger peppas model, formula (11)[36].

$$\ln(1 - M_t/M_0) = -K_1 t \quad (9)$$

$$M_t/M_0 = K_2 t^{1/2} \quad (10)$$

$$M_t/M_0 = K_n t^n \quad (11)$$

Here M_t is the drug release at time t , M_0 is the total drug content contained in the microspheres, and n is the constant.

2.3. Characterization

The scanning electron micrographs (SEM) were obtained on a SU8010 Ultra-High-Resolution SEM (Hitachi Company, Japan) at an Accelerating Voltage of 500 V. FT-IR characterization was carried out using a Nicolet (USA) IR200 Fourier transform infrared spectrometer with a scan range of $400\text{--}4000\text{ cm}^{-1}$, a resolution of 4 cm^{-1} , and a scan count of 32. Nexera UHPLC/HPLC system high performance liquid chromatograph, Shimadzu enterprise management (China) Co., Ltd (Disodium hydrogen phosphate (8 mmol/L, pH = 2.5) was used as the aqueous phase, acetonitrile as the organic phase, the wavelength was 210 nm, and the injection volume was 20 μL , the total flow rate is 1.2 mL/min (disodium hydrogen phosphate and acetonitrile flow rates are 0.6 mL/min respectively); Shanghai Tuofen Machinery Equipment Co., Ltd. is used for freeze-drying. The X-ray polycrystalline diffraction (XRD) were recorded with a X-ray polycrystalline diffractometer (Germany Brooke Co., Ltd.).

Determination of morphology and particle size of microspheres: SA/CS Ms or 4A/SA/CS Ms obtained above were randomly selected and arranged in close rows to measure the total diameter D of 15 microspheres with a ruler, subsequently calculate the average particle diameter.

3. Results and discussion

The synthesis of 4A/SA/CS Ms and SA/CS Ms as well as its drug loading and release were schematically shown in Fig. 1. Firstly, sodium alginate and 4A zeolite are completely mixed into the calcium chloride solution to calcification, and then put them into chitosan solution to obtain the final 4A/SA/CS Ms. For comparison, the SA/CS Ms was prepared in a same way except for the absence of 4A zeolite addition. In the next step, the influence of parameters such as 4A/SA/CS Ms content, SV concentration, temperature and pH on the adsorption process has been examined. The adsorption mechanism has been evaluated from adsorption isotherms and adsorption kinetics models. Finally, two kinds of drug loaded microspheres were used to investigate the release property toward SV in order to find which is suitable for using as sustained-release carrier.

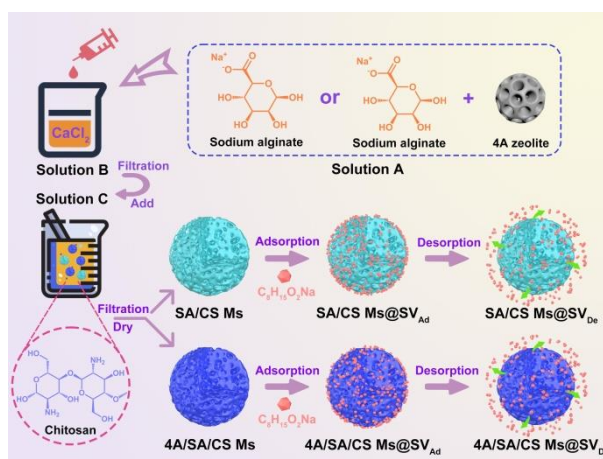


Fig. 1. Schematic diagram of microsphere synthesis and drug loading.

3.1. Particle size

The microspheres exhibit different degrees of particle size shrinkage and appearances under their respective drying methods.

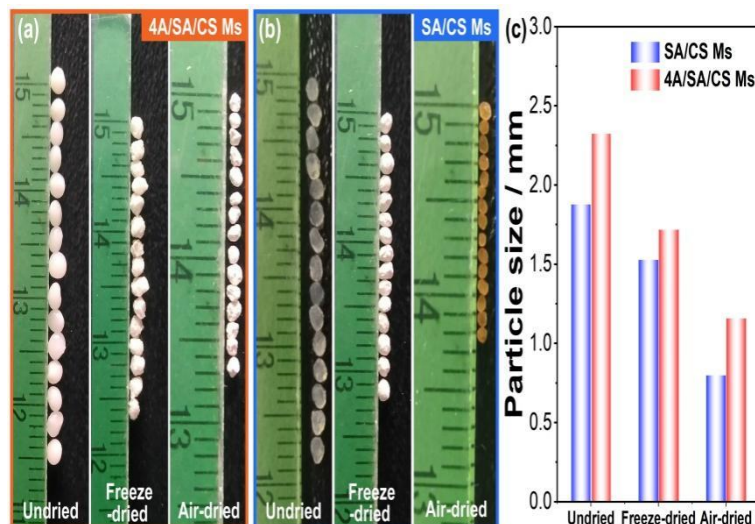


Fig. 2. The appearance (a, b) and corresponding size (c) of 4A/SA/CS Ms, and SA/CS Ms in different drying methods.

As shown in Fig. 2 and Fig. 3b, the 4A/SA/CS Ms were milky white and structural integrity, while the SA/CS Ms were transparent and light yellow. After freeze-dried, SA/CS Ms appear white and oblate shape (Fig. 4b). It was apparent that the volume of freeze-dried Ms (Fig. 2a. and Fig. 2b) was larger than that of air-dried, which can better maintain the microsphere morphology. Interestingly, with the addition of 4A zeolite, the particle size (Fig. 2c) of the spherical was augmented (the particle size of undried SA/CS Ms is 1.88 mm, 1.53 mm after freeze-dried, and 0.80 mm after air-dried, while for 4A/SA/CS Ms, the corresponding particle sizes are 2.33 mm, 1.72 mm, and 1.16 mm, respectively), which could be ascribed to the skeletal support property and dense structure of 4A zeolite.

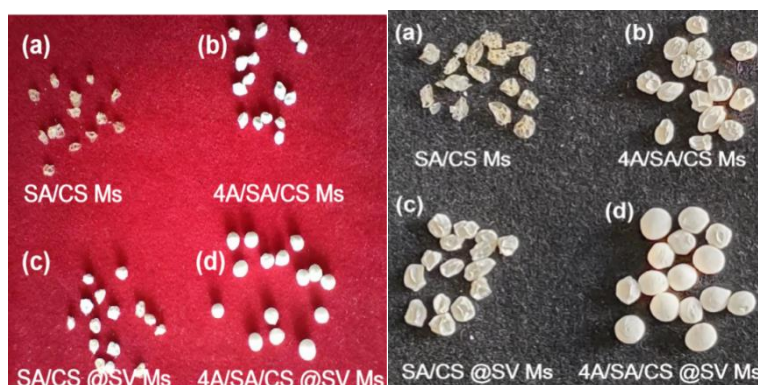


Fig. 3. Appearance (a, b, c, d) of 4A/SA/CS Ms, SA/CS Ms, 4A/SA/CS@SV Ms, SA/CS@SV Ms (freeze-dried). The microspheres in red background is prepared for the first time. The microspheres in black background is prepared for the second time.

Furthermore, it can also be seen from Fig. 3c and Fig. 3d that 4A zeolite increase the particle size of drug loaded microspheres remarkably. So we think that the addition of 4A zeolite improves the sphericity of microsphere and prevents the surface depression of the microspheres, thus expanding the specific surface area of the microspheres and increasing the adsorption sites inside the microspheres[37-38].

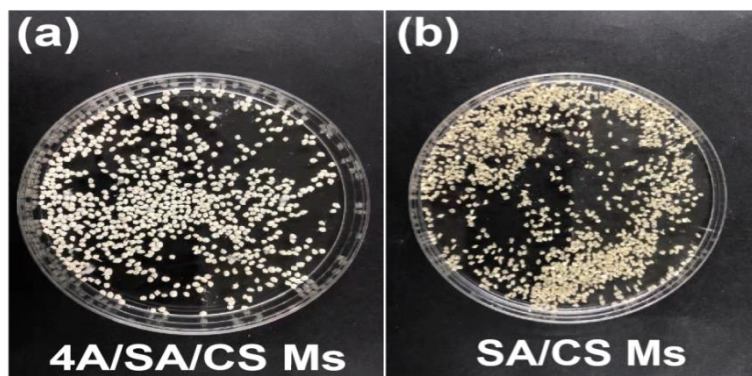


Fig. 4. Appearance (a, b) of 4A/SA/CS Ms and SA/CS Ms (freeze-dried).

3.2. SEM characterization

To inspect the microstructure of the the two microspheres, as revealed in Fig. 5a and Fig. 5c, both freeze-dried and air-dried 4A/SA/CS Ms samples show spherical structure. Fig. 5b and Fig. 5d showed the morphology of 4A/SA/CS Ms@SV and it can be seen that the spherical appearance were maintained except for shrinkage in volume and folds on the surface. In sharp contrast to 4A/SA/CS Ms, the air-dried SA/CS Ms without 4A zeolite addition were flattened and concave in Fig. 5e, while the freeze-dried SA/CS Ms were slightly smooth in Fig. 5g. Similarly, the surface of SA/CS Ms@SV (Fig. 5f and Fig. 5h) also contracted and folded. Comparing the microspheres in different states in Fig. 4a, it can be seen that the regular crystal porous structure of zeolite 4A plays a supporting role in the microsphere system, enhances the density of the microspheres, and significantly increases the volume of the microspheres. Based on the above analysis, it shows that the addition of 4A zeolite is beneficial to the formation and morphology of microspheres[39-40].

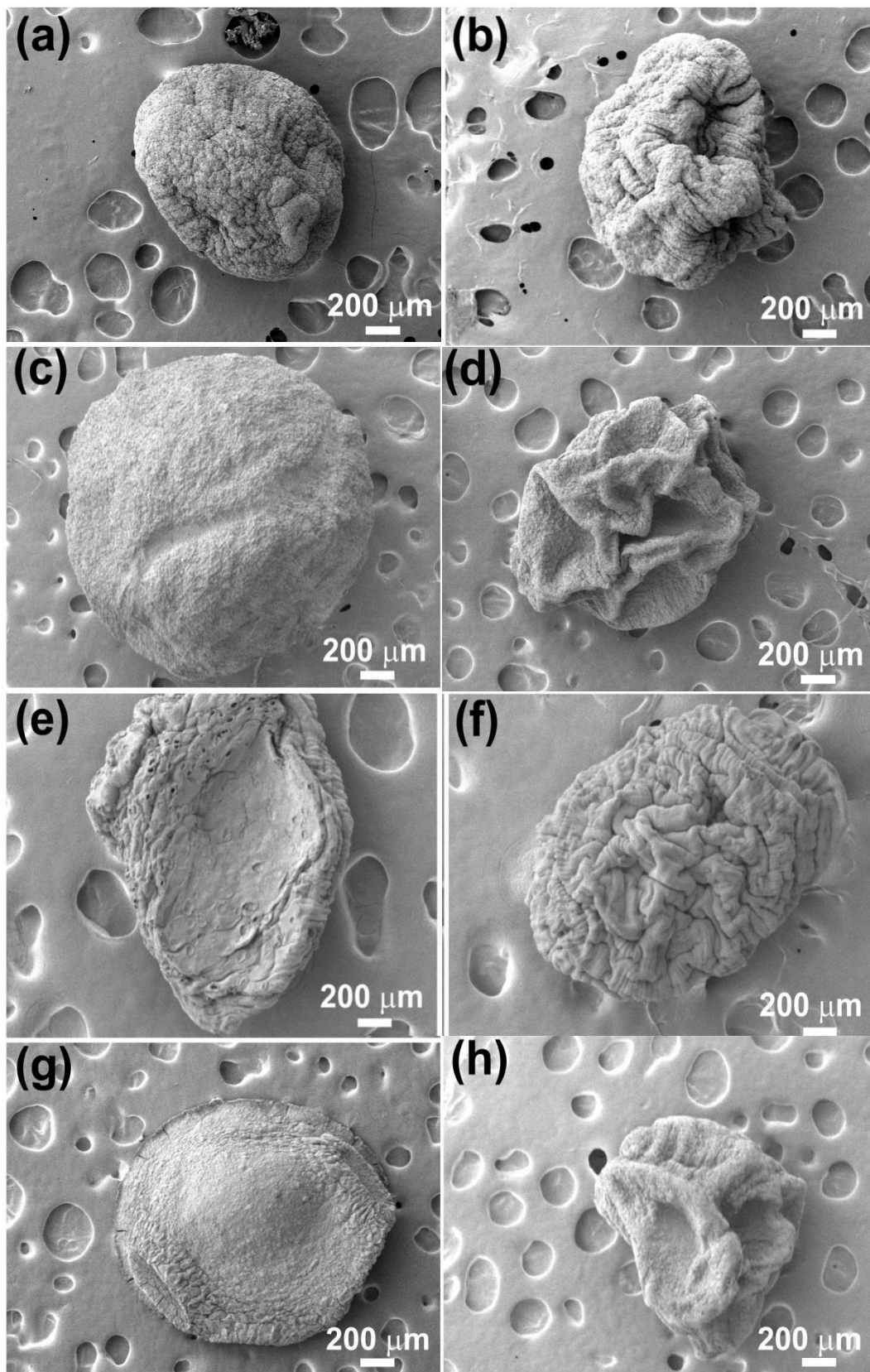


Fig. 5. SEM images of air-dried (a, b, e and f) and freeze-dried (c, d g and h) samples. (a, c) 4A/SA/CS Ms, (b, d) 4A/SA/CS Ms@SV, (e, g) SA/CS Ms, and (f, h) SA/CS Ms@SV_{Ad}.

3.3. FTIR analysis and XRD

Fig. 6a shows the Fourier transform infrared (FT-IR) spectra of 4A zeolite, SV, SA/CS Ms, SA/CS@SV Ms and 4A/SA/CS@SV Ms. In general, the FT-IR spectra of 4A zeolite samples showed feature peaks at 550 cm^{-1} for the double quaternary ring vibration, which is also observed in the spectrum of 4A/SA/CS Ms@SV. But it does not appear in the spectrum of SA/CS Ms and SA/CS@SV Ms (green dashed box in Fig. 6a), indicating that 4A zeolite is blended with sodium alginate and chitosan to form microspheres, but no new chemical bonds are formed. The characteristic peak at 1417 cm^{-1} in the SV spectrum can be ascribed to the symmetric stretching vibration of the carboxylate -COO^- [41-42]. As expected, the intensities of the feature peak appears in the spectra of both 4A/SA/CS@SV Ms and SA/CS@SV Ms, meaning that SV is successfully adsorbed into the microsphere matrix. The structure of the obtained samples was also investigated by XRD. In Fig. 6b, it is revealed that difference in crystallinity of two types samples (with or without 4A zeolite) can be observed. The diffraction peaks of SA/CS Ms and SA/CS@SV Ms were dispersive, which proves the poor crystallinity of these two samples. Interestingly, the diffraction signals of 4A/SA/CS Ms and 4A/SA/CS@SV Ms shown that the products has high crystallinity, the corresponding diffraction peaks belong to the simple cubic structure of 4A zeolite (JCPDS No. 89-3859), which indicates that 4A zeolite is successfully incorporated into the microspheres.

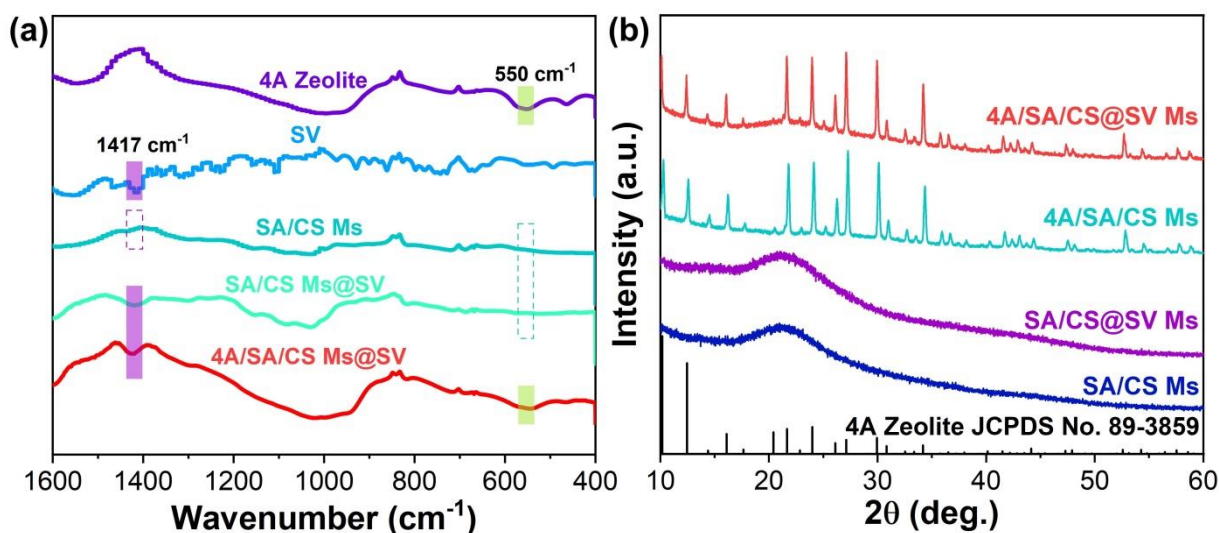


Fig. 6. (a) FT-IR spectra of 4A zeolite, SV, SA/CS Ms, SA/CS@SV Ms and 4A/SA/CS@SV Ms. (b) XRD patterns of 4A zeolite, SA/CS Ms, SA/CS@SV Ms, 4A/SA/CS Ms, 4A/SA/CS@SV Ms.

3.4. Adsorption study

The adsorption behavior toward SV was evaluated by using both 4A/SA/CS Ms and SA/CS Ms. The mass concentration of SV can be calculated through the equation of Fig. 7. Through the above experiments and characterization, the microspheres obtained by air-dried are unstable and easy to break (Fig. 3a), for this reason freeze-dried microspheres are used in the following adsorption and desorption experiments.

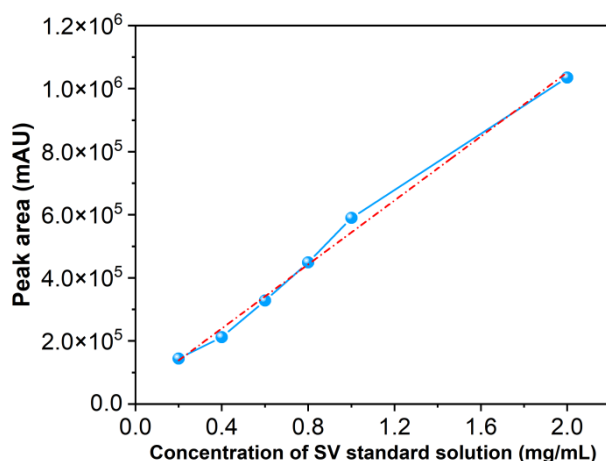


Fig. 7. Standard curve of SV.

It was observed in Fig. 8 that both of the two microspheres have comparatively powerful adsorption ability for SV. As depicted in Fig. 8a, the adsorption capacity of 4A/SA/CS Ms or SA/CS Ms followed the same trend, both of which increased first and then decreased with temperature, and the optimal absorption amount of SV by 4A/SA/CS Ms was found to be 8.1833 mg/g at 25 °C.

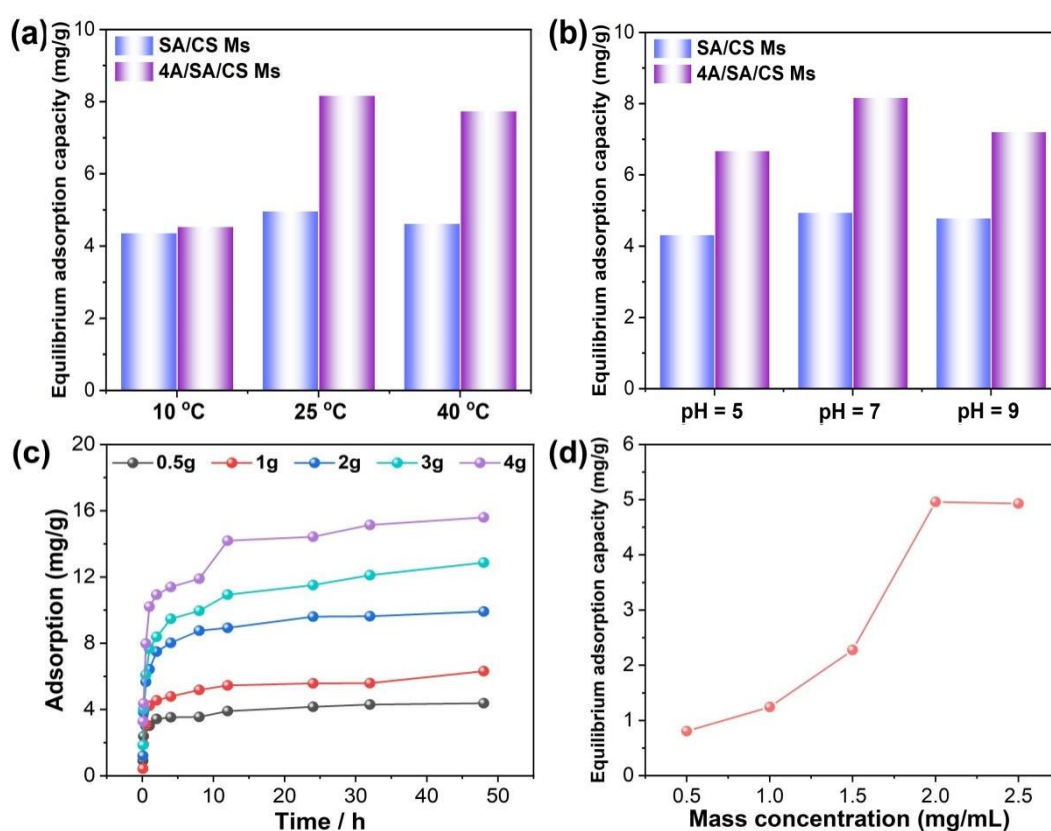


Fig. 8. Equilibrium adsorption capacity of SA/CS Ms and 4A/SA/CS Ms for SV at (a) different temperatures, (b) different pH. Adsorption conditions: (a) pH = 7, 2 g Ms, (b) 25 °C 2 g Ms. (c) Equilibrium adsorption capacity of SV with different dosage of 4A/SA/CS Ms. pH = 7, 25 °C (d) Equilibrium adsorption capacity of SV with different concentration of SV. pH = 7, 25 °C.

The reason may be that high or low temperature inhibits the swelling of the microspheres, so it increases the adsorption resistance. Under the same conditions, the equilibrium adsorption capacity of 4A/SA/CS Ms is higher than that of SA/CS Ms which is due to the framework support property of 4A zeolite and its abundant channels with uniform pore size in the crystal[43-44]. Combined with the SEM characterization and adsorption data, it can be deduced that 4A zeolite can promote the formation, morphology and adsorption properties of microspheres.

Furthermore, the pH of aqueous solution also affect the adsorbate strength. As shown in Fig. 8b, the equilibrium adsorption capacity of SA/CS MS for SV increases with the increase of pH, but decreases when the $\text{pH} > 7$. This may be related to the pK_a of sodium alginate and chitosan. Under acidic conditions, the carboxyl group of sodium alginate combines with hydrogen ions to form carboxylic acids, weakening the intermolecular force, resulting in small morphological changes; while in alkaline environment, chitosan will precipitate and solidify, and shrinking the structure, inhibiting the swell of microspheres[45-46]. When $\text{pH} = 7$, the larger swelling rate of microspheres leads to the maximum adsorption of SV. The maximum q_e values of SA/CS Ms toward SV at $\text{pH} = 7$ is 4.9776 mg/g, corresponding adsorption capacity of 4A/SA/CS MS for SV is 8.1833 mg/g, indicating drug loaded could be affected by the addition of 4A zeolite notably. So, we have the reason to believe that 4A zeolite can effectively inhibit the excessive swelling of Ms and reduce the swelling rupture of microspheres because of its stable structure.

As can be seen from Figure 8c, the adsorption rate of 4A/SA/CS Ms for SV was faster in 0-2 h, while the adsorption close to the equilibrium after 4 h owing to the active sites available reduced. Meanwhile, the adsorption capacity has positive correlation with 4A/SA/CS Ms amount. It can be seen that when the concentration of SV is above 2.0 mg/mL, the adsorption tends to be stable (Fig 8d) by 4A/SA/CS Ms which may be the saturation of the adsorption sites inside 4A/SA/CS Ms. Therefore, the concentration of SV was fixed at 2.0 mg/mL in our adsorption and desorption experiments.

Thermodynamic parameters for the adsorption were calculated from the variations of the thermodynamic equilibrium constant K_d by plotting of $\ln K_d$ versus $1/T$ (Fig. 9). Then the slope and intercept were used to determine the values of ΔH and ΔS , and the Van't Hoff equation was applied to calculate Gibbs free energies ΔG (Table 1). The free energy ΔG of the process were negative which indicate that the adsorption process is spontaneous. According to the ΔS results presented we can know that the adsorption of SV by SA/CS Ms and 4A/SA/CS Ms resulted in the creation of steric hindrance which reflected by the increased entropy values in the system. The adsorption of SV by the two microspheres has a negative enthalpy change, which shows that low temperature is more conducive to the adsorption process.

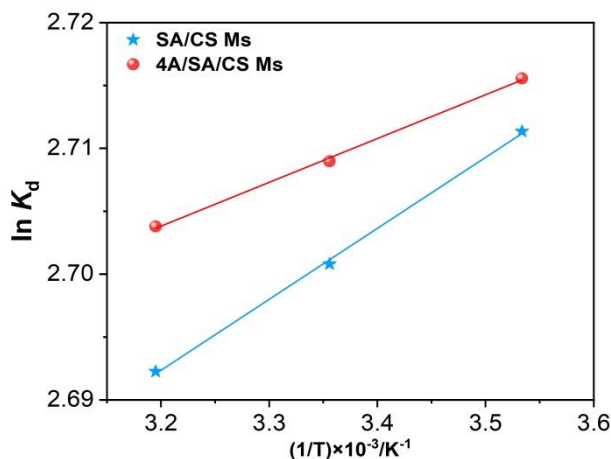


Fig. 9. Van't Hoff plot for SV adsorption.

In order to gain insight into the adsorption mechanism, three mathematical equations, according to the formula (1-3). The adsorption data were further analyzed shown in Table 1.

Table 1. Thermodynamic parameters of sodium valproate adsorption by different microspheres at different temperatures.

Microsphere	ΔH (kJ/mol)	ΔS ($J \cdot mol^{-1} \cdot K^{-1}$)	ΔG (kJ/mol)		
			283K	298K	313K
SA/CS	-0.4689	22.5404	-6379.4099	-6718.6696	-7006.0195
4A/SA/CS	-0.2893	22.5762	-6389.3414	-6698.7614	-7036.5413

The adsorption kinetics are important to evaluate the adsorbent efficiency and help to understand the mechanism of adsorption. From pseudo-first-order model (4) and pseudo-second-order model (5), the equilibrium adsorption capacity and adsorption rate constant during the adsorption was calculated. Based on the $\log(q_e - q_t) \sim t$ and $t/q_t \sim t$ curves in Fig. 10, both of two microspheres have good dynamic linearity and the adsorption kinetic constant were calculated.

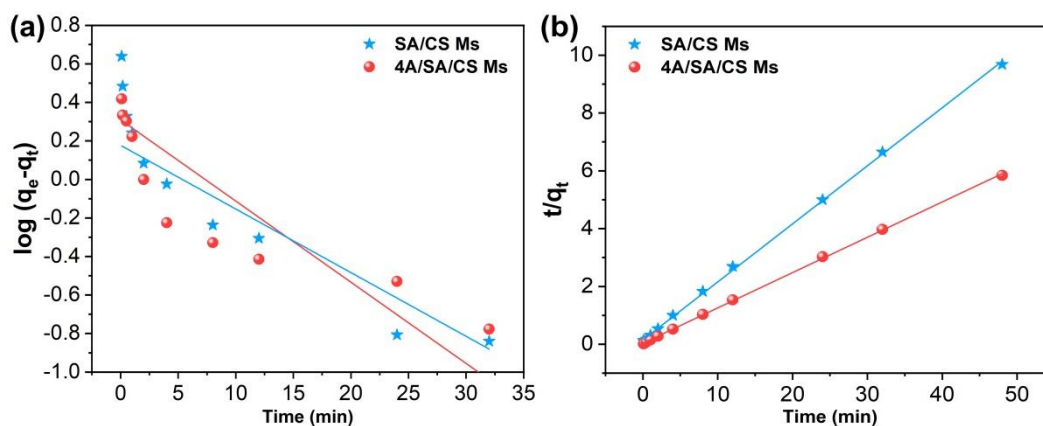


Fig. 10. The Pseudo-first order kinetics (a) and Pseudo-second order kinetics (b) for SV.

Based on the data we can know that the correlation coefficient of the pseudo second order equation ($R_2^2 \geq 0.9947$) is greater than that of the pseudo first order equation ($R_1^2 \leq 0.9126$), which shows that the process of SA/CS Ms adsorbing SV is more in line with the pseudo second order model. Consequently, it can be inferred that the process of SA/CS Ms adsorbing SV is a chemical adsorption process. Moreover, from Table 2 we also know that for 4A/SA/CS Ms the adsorption should be a physical adsorption of multiple molecular layers[47].

Table 2. Kinetic parameters of sodium valproate adsorption by two Ms.

	Pseudo-first order model			Pseudo-second order model		
	$k_1(\text{h}^{-1})$	$q_e(\text{mg/g})$	R_1^2	$k_2(\text{h}^{-1})$	$q_e(\text{mg/g})$	R_2^2
SA/CS Ms	0.0914	3.3612	0.9126	0.1523	8.7796	0.9986
	0.0532	2.7058	0.6414	0.1512	6.1538	0.9947
4A/SA/CS Ms	0.1780	4.2772	0.9969	0.0696	2.1125	0.8503
	0.2531	3.9108	0.9978	0.0891	1.8690	0.8931

Equilibrium isotherms can provide useful information about adsorption mechanism, among which Langmuir and Freundlich isotherms are the most commonly used. The Langmuir and Freundlich models are expressed by equation (6) and equation (7), respectively. Adsorption parameters of 4A/SA/CS Ms are calculated respectively are shown in Table 3. Correlation coefficient of Freundlich equation ($R_F^2 = 0.8837$) is greater than that of Langmuir equation ($R_L^2 = 0.3429$), so it is expected that, the adsorption process of SV on 4A/SA/CS Ms conforms to Freundlich model, that is, the adsorption of SV on 4A/SA/CS Ms belongs to non ideal adsorption.

Table 3. Isothermal adsorption parameters of sodium valproate by 4A/SA/CS Ms.

Temperature	Langmuir equation			Freundlich equation		
	$q_{\max}(\text{mg/g})$	K_L	R_L^2	k_F	n	R_F^2
298K	6.0864	0.1974	0.3429	1.6104	0.8053	0.8837

3.5. Effect on desorption of SA/CS Ms@SV and 4A/SA/CS Ms@SV

As shown in Fig.11b, the release profiles of SV from 4A/SA/CS Ms@SV or SA/CS Ms@SV with the temperature range from 10 °C to 40 °C was discussed. From the data, it can be seen that 25 °C is more suitable for desorbing SV by 4A/SA/CS Ms@SV or SA/CS Ms@SV. In the same test conditions the cumulative release percentage of SA/CS Ms@SV reached 38.06% (red dotted line) while 4A/SA/CS Ms@SV reached 42.69% (red solid line) which is due to the three-dimensional skeleton structure composed of silica and alumina tetrahedron[48-49]. So we can know that the addition of 4A zeolite not only increases the number of orifices, but also provides more paths for SV molecular diffusion and simultaneously profit by the physical adsorption of multiple molecular layers, the binding force between SV molecules and microspheres is weak, which is easier to desorption.

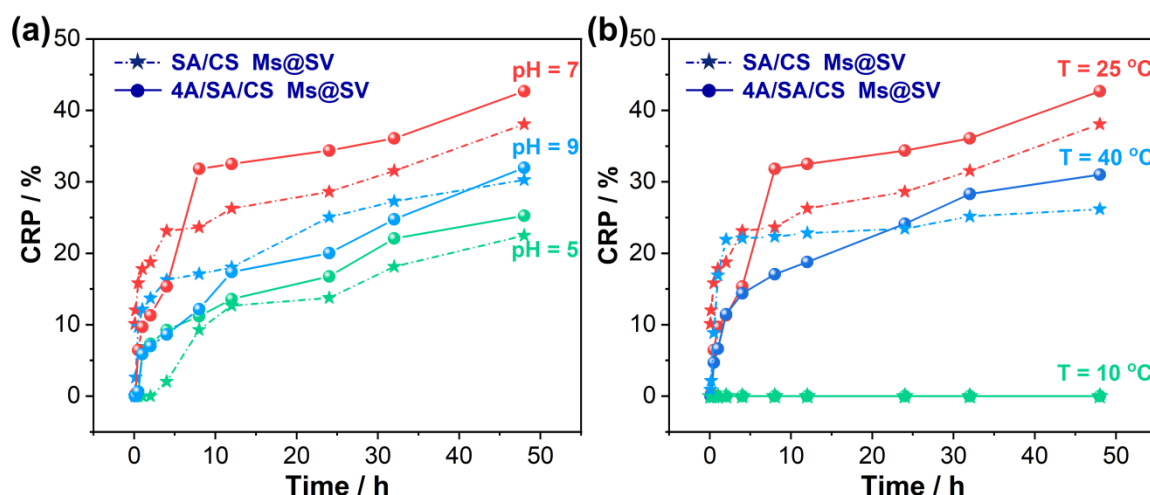


Fig. 11. Cumulative release percentage of 4A/SA/CS Ms@SV and SA/CS Ms@SV at different conditions. (a) pH (b) temperature.

The pH value of the solution is a crucial factor affecting desorption. When the temperature was fixed at 25 °C, the release percentage of SV from 4A/SA/CS Ms@SV and SA/CS Ms@SV was discussed ranging of pH from 5 to 9 in Fig. 11a. The OH⁻ ions in the alkaline solution and -COO⁻ form hydroxide precipitation[50-51], which hinders the desorption. So SA/CS Ms@SV Ms and 4A/SA/CS Ms@SV Ms occurs the strongest ability to release SV at pH = 7. Moreover, compare the desorption performance of the two microspheres, at 25 °C and pH = 7, the results shows that the cumulative release percentage of 4A/SA/CS Ms@SV Ms keep higher than that of SA/CS Ms@SV Ms. 4A/SA/CS Ms, as the delivery carrier of SV, use its own swelling and advantage of 4A zeolite to regulate its release, so SV can be released slowly at a stable and controllable rate. We infer that 4A/SA/CS Ms@SV Ms have better slow and controlled release performance and maintain high efficiency for the release of SV.

As shown in Table 4, the kinetic parameters of SV release from the two microspheres are calculated according to the above three models. We can ascertain that under the conditions of 25 °C and pH = 7, the correlation coefficient (R_n^2) of Riger peppas model > the correlation coefficient (R_h^2) of Higuchi equation > the correlation coefficient (R_1^2) of the first-order drug release formula. Thus, it can be inferred that the process of SV release from the two microspheres conforms to the Riger peppas model. In addition, it can be seen that n is less than 0.43 for both microspheres during the release of SV, so the drug release from both microspheres belongs to Fick diffusion[52-54].

Table 4. Kinetic parameters of sodium valproate release from microspheres.

	First order release equation		Higuchi equation		Riger-Peppas equation		
	K_1	R_1^2	K_2	R_h^2	K_n	n	R_n^2
4A/SA/CS Ms@SV	0.0059	0.8887	0.0374	0.9612	0.0582	0.3587	0.9752
SA/CS Ms@SV	0.0066	0.8745	0.0362	0.9461	0.169	0.1873	0.9823

4. Conclusions

In summary, two kinds of microspheres containing 4A zeolite or not and its SV loaded microspheres were prepared. The morphological characterizations show that the addition of 4A zeolite can increase the particle size of SA/CS Ms. Furthermore the steric structure of freeze-dried microspheres is better than that of air-dried microspheres. Through the study of 4A/SA/CS Ms adsorption performance for SV, it is found that the adsorption conforms to non ideal adsorption and the addition of 4A zeolite can increase the adsorption capacity. It is shown that the adsorption is a spontaneous process and the maximum adsorption capacity toward SV by 4A/SA/CS Ms reach 8.1833 mg/g. Release experiments of 4A/SA/CS Ms@SV at different condition showed that the release of SV belonged to Fick diffusion. Therefore, these obtained results illustrate the advantages of adsorption and release capacity of 4A/SA/CS Ms which may offer suitable approaches for the preparation of new controlled drug delivery systems for agrochemical applications to improve pesticide stability and persistence.

Acknowledgements

This work was supported by the National Natural Science Foundation of Shandong Province (ZR2020MC129, ZR2014CM039), Shandong Province Science and technology-based maximum innovation capacity improvement project(2022TSGC1311), and Shangdong Province Major Project of Agricultural Application Technology and Innovation (SD2019ZZ002).

References

- [1] M. Zhao, H. Zhou, L. Chen, L. Hao, H. Chen, X. Zhou, *Carbohydrate Polymers*. 243, 116433(2020); <https://doi.org/10.1016/j.carbpol.2020.116433>
- [2] I. Ravier, E. Haouisee, M. Clement, R. Seux, O. Briand, *Pest Management Science*. 61(8), 728(2005); <https://doi.org/10.1002/ps.1049>
- [3] M. O. Jibrin, Q. C. Liu, J. B. Jones, S. A. Zhang, *Plant Pathology*, 70, 495(2021); <https://doi.org/10.1111/ppa.13318>
- [4] J. Li, H. Q. Li, C. H. Guo, *Fine and Specialty Chemicals*, 24(12), 44(2016).
- [5] S. F. Yang, H. N. Zhang, H. Xu, *Chinese Journal of Hospital Pharmacy*, 25(5), 434(2005).
- [6] S. J. Deepak, S. Gunta, S. Mallika, S. Pranav, *Talanta*. 72(1), 80(2007); [https://doi.org/10.1016/S0039-9140\(07\)00459-6](https://doi.org/10.1016/S0039-9140(07)00459-6)
- [7] L. M. Song, W. X. Liang, B. N. Lv, D. L. Li, CN104904715A, (2015).
- [8] L. J. Lovett, G. A. Nygard, G. R. Erdann, C. Z. Burley, S. K. Wahba Khalil, *Journal Liquid Chromatogr.* 10(4), 687(1987); <https://doi.org/10.1080/01483918708069019>
- [9] D. M. Ijff, A. P. Aldenkamp, *Handbook of clinical neurology*. 111, 707(2013); <https://doi.org/10.1016/B978-0-444-52891-9.00073-7>
- [10] W. Loscher, *CNS Drugs*. 16(10), 669(2002); <https://doi.org/10.2165/00023210-200216100-00003>
- [11] L. Davis, A. Bartolucci, F. Petty, *Journal of Affective Disorders*. 85(3), 259(2005); <https://doi.org/10.1016/j.jad.2004.09.009>

- [12] A. M. Helmiyati, IOP Science. 188(1), 1(2017); <https://doi.org/10.1088/1757-899X/188/1/012019>
- [13] C. Y. Zhang, G. H. He, X. M. Yan, Functional materials. 41(12), 2153(2010).
- [14] J. Kozłowska, W. Prus, N. Stachowiak, International Journal of Biological Macromolecules. 129, 952(2019); <https://doi.org/10.1016/j.ijbiomac.2019.02.091>
- [15] S. Maiti, K. Singha, S. Ray, P. Dey, B. Sa, Pharmaceutical Development and Technology. 14(5), 461(2009); <https://doi.org/10.1080/10837450802712658>
- [16] T. Chaki, N. Kajimoto, H. Ogawa, T. Baba, N. Hiura, Bioscience, Biotechnology, and Biochemistry. 71(8), 1819(2007); <https://doi.org/10.1271/bbb.60620>
- [17] Y. Ma, S. Li, T. Ji, W. Wu, D. E. Sameen, S. Ahmed, Carbohydrate Polymers, 247, 116738(2020); <https://doi.org/10.1016/j.carbpol.2020.116738>
- [18] V. K. Mourya, N. N. Inamdar, Reactive and Functional polymers. 68(6), 1013(2008); <https://doi.org/10.1016/j.reactfunctpolym.2008.03.002>
- [19] F. Scalera, F. Gervaso, V. M. D. Benedictis, M. Madaghiele, C. Demitri, IEEE Transactions on Nanotechnology. 15(6), 884(2016); <https://doi.org/10.1109/TNANO.2016.2573923>
- [20] F. H. Li, X. R. Zhang, L. Y. Xiang, New Chemical Materials, 44(1), 31(2016).
- [21] I. Younes, M. Rinaudo, Marine Drugs. 13(3), 1133(2015); <https://doi.org/10.3390/md13031133>
- [22] F. Xiang, H. Q. Yan, X. Q. Chen, New chemical materials, 44(2), 165(2016).
- [23] J. D. Wang, R. R. Wang, Journal of hebei Agricultural Science, 12(2), 12(2008).
- [24] Z. H. Li, G. L. Liang, J. Guan, New chemical materials. 43(6), 77(2015).
- [25] T. Z. Yang, W. M. Zhang, H. Y. Liu, Y. N. Guo, Journal of Radioanalytical and Nuclear Chemistry. 323(2), 1(2019); <https://doi.org/10.1007/s10967-019-06993-w>
- [26] M. E. Davis, Nature. 417(6891), 813(2002); <https://doi.org/10.1038/nature00785>
- [27] A. Martucci, L. Pasti, M. Nassi, A. Alberti, R. Arletti, R. Bagatin, Microporous & Mesoporous Materials. 151(11), 358(2012); <https://doi.org/10.1016/j.micromeso.2011.10.010>
- [28] S. Kumar, R. Bera, N. Das, J. Koh, Carbohydrate Polymers, 232, 115808(2020); <https://doi.org/10.1016/j.carbpol.2019.115808>
- [29] Q. Z. Zhang, Y. Du, M. L. Yu, L. R. Ren, Y. F. Guo, Q. H. Li, Carbohydrate Polymers, 277, 118880(2022); <https://doi.org/10.1016/j.carbpol.2021.118880>
- [30] Y. Zhang, L. Q. Zhang, X. J. Jiao, B. H. Zhang, Fine Chemicals, 36(3), 387(2019).
- [31] L. Tang, Value Health, 18(3), 277(2015); <https://doi.org/10.1016/j.jval.2015.03.1622>
- [32] X. Li, D. L. Zeng, Z. Y. He, P. Ke, Y. S. Tian, G. H. Wang, Carbohydrate Polymers, 276, 118729(2022); <https://doi.org/10.1016/j.carbpol.2021.118729>
- [33] Y. Y. Yang, L. Zeng, Z. K. Lin, H. B. Jiang, A. P. Zhang, Carbohydrate Polymers, 274, 118622(2021); <https://doi.org/10.1016/j.carbpol.2021.118622>
- [34] Q. W. Lin, M. F. Gao, J. L. Chang, H. Z. Ma, Carbohydrate Polymers, 151, 283(2016); <https://doi.org/10.1016/j.carbpol.2016.05.064>
- [35] Q. Y. Zhang, J. Tong, W. Zhou, Z. B. Zhong, Q. C. Hu, Q. Ma, H. T. Long, S. Q. Wu, X. W. Shi, Q. F. Ye, Carbohydrate Polymers, 287, 119326(2022); <https://doi.org/10.1016/j.carbpol.2022.119326>

- [36] S. I. Lyubchik, A. I. Lyubchik, O. L. Galushko, L. P. Tikhonova, J. Vital, I. M. Fonseca, S. B. Lyubchik, *Colloids and Surfaces A: Physicochem. Eng. Aspects*, 242, 151(2004); <https://doi.org/10.1016/j.colsurfa.2004.04.066>
- [37] D. Verboekend, G. Vilé, J. Pérez-Ramírez, *Advanced Functional Materials*. 22, 916(2012); <https://doi.org/10.1002/adfm.201102411>
- [38] L. Duan, Y. Wang, Y. Zhang, *International Journal of Polymeric Materials and Polymeric Biomaterials*, 67(5), 288(2018); <https://doi.org/10.1080/00914037.2017.1323215>
- [39] R. Sabarish, G. Unnikrishnan, *Carbohydrate Polymers*, 199, 129(2018); <https://doi.org/10.1016/j.carbpol.2018.06.123>
- [40] J. K. Zhang, Q. L. Huang, Y. Wu, *Chinese Journal of Pesticide Science*, 22(2), 225(2020).
- [41] B. Zhou, J. Zhao, *Fine Chemical*, 25(7), 625(2008).
- [42] R. H. Hui, C. X. Guan, D. Y. Hou, *Journal of Anshan Teachers College*. 3(1), 95(2001).
- [43] J. An, S. J. Geib, N. L. Rosi, *Journal of the American Chemical Society*. 131(24), 8376(2009); <https://doi.org/10.1021/ja902972w>
- [44] H. Hayashi, A. P. Cote, H. Furukawa, M. O'Keeffe, O. M. Yanghi, *Nature Materials*. 6, 501(2007); <https://doi.org/10.1038/nmat1927>
- [45] G. K. Thirunavukkarasu, G. Nirmal, H. Lee, *Journal of Industrial and Engineering Chemistry*, 69(1), 405(2019); <https://doi.org/10.1016/j.jiec.2018.09.051>
- [46] C. Xu, L. Cao, M. Bilal, C. Cao, P. Zhao, H. Zhang, *Carbohydrate Polymers*, 262, 117933(2021); <https://doi.org/10.1016/j.carbpol.2021.117933>
- [47] W. Zhang, J. Y. Song, Q. L. He, H. Y. Wang, W. L. Iyu, H. J. Feng, *Journal of Hazardous Materials*. 384, 121445(2020); <https://doi.org/10.1016/j.jhazmat.2019.121445>
- [48] C. Isha, S. Nimrata, A.C. Rana, *International Research Journal of Pharmacy*, 3(5), 57(2012).
- [49] P. Mukhopadhyay, K. Sarkar, S. Bhattacharya, *Carbohydrate Polymers*, 112, 627(2014); <https://doi.org/10.1016/j.carbpol.2014.06.045>
- [50] S. Ouerghemmi, S. Dimassi, N. Tabary, *Carbohydrate Polymers*, 196, 8(2018); <https://doi.org/10.1016/j.carbpol.2018.05.025>
- [51] L. Wang, D. M. Cheng, H. H. Xu, *Journal of South China Agricultural University*, 3, 53(2011).
- [52] M. C. Camara, E.V. Campos, R. A. Monteiro, *Journal of Nanobiotechnol.* 17(1), 100(2019); <https://doi.org/10.1186/s12951-019-0533-8>
- [53] B. D. Mattos, B. L. Tardy, W. L. E. Magalhaes, O. J. Rojas, *Journal of Controlled Release*, 262, 139(2017); <https://doi.org/10.1016/j.jconrel.2017.07.025>
- [54] L. L. Huang, W. P. Sui, Y. X. Wang, *Carbohydrate Polymers*, 80, 168(2010); <https://doi.org/10.1016/j.carbpol.2009.11.007>